



BIOT DYNAMIC CONSOLIDATION FINITE ELEMENT ANALYSIS USING A HYPO-PLASTICITY MODEL

Cheng ZHOU¹, Zhu-Jiang SHEN² and Jian-Hua YIN³

SUMMARY

Equivalent viscous elastic models, which are not very realistic for soils, have been proposed and implemented into dynamic consolidation analyses for several decades. Elastic plastic models are better for soils. However these models have not been used successfully in the analyses of dynamic Biot consolidation. The main reason is that a great amount of work must be done by formulating the inverse stiffness matrix $[K]^{-1}$ in each small Δt step if using an implicit finite difference scheme. In order to save work of calculation, an explicit finite difference scheme may be used for elastic plastic analyses of the dynamic response of a soil foundation. But, due to the ill condition for solution to the permeability matrix by using a small Δt such as 10^{-6} to 10^{-5} second, the uncoupling between dynamic equilibrium and permeability equations in Biot dynamic consolidation theory is difficult to fulfill. Therefore, an asynchronous staggered iteration method with an explicit difference scheme is suggested. In this paper, a hypo-plasticity model is first presented and verified using triaxial tests on silty clays. The algorithm using a hypo-plasticity model is implemented in a finite element (FE) code based on Biot dynamic consolidation theory. The dynamic solid-liquid coupling elastic plastic responses of a saturated sand foundation are analyzed and reasonable results are achieved.

INTRODUCTION

Equivalent viscous elastic models and linear methods have been proposed and implemented into dynamic nonlinear consolidation analyses of soils for several decades [1-2]. However, the equivalent viscous elastic models are not very realistic for soils, although the average shear modulus, damp ratio and empirical formulas for permanent volumetric and deviatoric strains and porewater pressure can be easily derived using these models when they are implemented in the equivalent linear dynamic consolidation analysis. Under complex loading and variable stress path, soils exhibit complicated stress-strain characteristics, which can not be modelled by the viscous elastic models. Sometimes the post-earthquake deformations of

¹ Senior Engineer, Nanjing Hydraulic Research Institute, Nanjing, 210024; Research Assistant and Part-time PhD Student, The Hong Kong Polytechnic University; China. Email: cheng.zhou@polyu.edu.hk

² Professor, Tsinghua University, China. Email: zjshen@tsinghua.edu.cn

³ Professor, The Hong Kong Polytechnic University, China. Email: cejhyin@polyu.edu.hk

geotechnical structures are larger than the results predicted using equivalent viscous elastic models and methods, for example, in San Francisco earthquake in 1971 [3]. Elastic plastic models are better for soils and can capture the complicated behavior of soils under complex loading and variable stress path. However these models have not been used successfully in the analyses of dynamic Biot consolidation. The main reason is that a great amount of work must be done by formulating the inverse stiffness matrix in each small Δt step when elastic plastic models and implicit finite difference scheme are used; while only one inverse stiffness matrix is needed to be formulated in each Δt step if equivalent viscous elastic models and equivalent linear method are used. In order to save work of calculation, an explicit finite difference scheme may be used for elastic plastic analyses of the dynamic response of a soil foundation. But, due to the ill condition for solution to the permeability matrix by using a small Δt such as 10^{-6} to 10^{-5} second, the uncoupling between dynamic equilibrium and permeability equations in Biot dynamic consolidation theory is difficult to fulfill [4-6]. Therefore, an asynchronous staggered iteration method with an explicit difference scheme is suggested in this paper. A hypo-plasticity model is proposed. The staggered iteration between an elastic model and the hypo-plasticity model makes it possible to determine the stress increment in the proposed algorithm based on Biot dynamic consolidation theory [7]. Using the hypo-plasticity model and asynchronous staggered iteration method, the dynamic solid-liquid coupling elastic plastic responses of a saturated sand foundation are analyzed and reasonable results are achieved.

THE HYPOPLASTICITY MODEL

A good reasonable model should be able to model not only the stress-strain behaviour of soils under simple loading, but also the stress-strain behaviour of soils under complicated loading. The model parameters should also be easily determined using conventional tests. In this section, a model is first developed for stress-strain behaviour of soils under simple loading, then the model is extended to model the complicated stress-strain behaviour of soils using the hypo-plasticity theory [8-9].

The incremental effective stress tensor is divided into two parts, *i.e.*, $d\sigma'_{ij} = p' d\gamma_{ij} + \sigma'_{ij} dp' / p'$, so that the mutual effects of spherical and deviator stress on the stress-strain behaviour of soils can be modelled. The deviator stress tensor is defined as $\gamma_{ij} = s_{ij} / p'$ and the scalar deviator stress ratio is defined as $\eta = \gamma_{ij} \alpha_{ij}$. α_{ij} is a tensor in the same direction as the incremental deviator stress ratio tensor $d\gamma_{ij}$. The definition of the stress tensor α_{ij} at the *n*-th step will be given in the following.

The strain can be divided into four parts: the volumetric strain ϵ_{vc} induced by compression, the volumetric strain ϵ_{vs} induced by shearing, the deviatoric strain ϵ_{sc} induced by compression and the deviatoric strain ϵ_{ss} induced by shearing [10-12]. In one dimensional or isotropic compression, we have

$$\begin{cases} d\epsilon_{vc} = \frac{0.434C_c}{1+e_0} \frac{dp'}{p'} = \frac{dp'}{K_c} \\ d\epsilon_{vc}^e = \frac{0.434C_s}{1+e_0} \frac{dp'}{p'} = \frac{dp'}{K_s} \end{cases} \quad (1)$$

Considering that $\Delta\epsilon_2 = \Delta\epsilon_3 = 0 \Rightarrow \Delta\epsilon_v = \Delta\epsilon_s = \Delta\epsilon_1$ in one dimensional compression, the deviatoric strain induced by compression is

$$\begin{cases} d\varepsilon_{sc} = \frac{\eta}{\eta_0} \frac{dp}{K_c} \\ d\varepsilon_{sc}^e = \frac{\eta}{\eta_0} \frac{dp}{K_s} \end{cases} \quad (2)$$

where η_0 is the earth pressure at rest. In shearing under constant spherical stress, we have

$$\varepsilon_{ss} = \frac{a\eta}{\eta_f - \eta} \quad (3)$$

where a is the inverse of the initial shear modulus G , η_f is the deviator stress ratio at failure. It is assumed that η_f increases linearly with contraction of soils, i.e.,

$$d\eta_f = c_f d\varepsilon_{vs} \quad (4)$$

where c_f is a scaling coefficient for the increase of η_f .

The incremental of $d\varepsilon_{ss}$ is

$$d\varepsilon_{ss} = \frac{a}{(\eta_f - \eta)^2} (\Delta\eta\eta_f - c_f\eta d\varepsilon_{vs}) \quad (5)$$

The linear dilation equation is assumed as

$$\frac{d\varepsilon_{vs}}{d\varepsilon_{ss}} = \frac{1}{\lambda} (\eta_d - \eta) \quad (6)$$

where λ and η_d are two dilation parameters.

Substituting Eqn. (6) into Eqn. (5), and using Eqn. (6), we can get

$$\begin{cases} d\varepsilon_{ss} = \frac{a}{g} d\eta \\ d\varepsilon_{vs} = \frac{a}{g} \frac{(\eta_d - \eta)}{\lambda} d\eta \end{cases} \quad (7)$$

$$\text{where } g = \frac{(\eta_f - \eta)^2}{\eta_f^2} + \frac{ac_f\eta}{\eta_f^2} \frac{\eta_d - \eta}{\lambda}$$

By now, the stress-strain relationship under simple loading can be written as

$$\begin{cases} d\varepsilon_v = \frac{dp}{K_c} + \frac{a}{g} \frac{(\eta_d - \eta)}{\lambda} d\eta \\ d\varepsilon_s = \frac{dp}{K_c} \frac{\eta}{\eta_0} + \frac{a}{g} d\eta \end{cases} \quad (8)$$

where a , c_f , K_c , K_s , λ , c_f , η_0 , η_d , η_f are eight parameters for the model.

In order to extend the stress-strain relationship under simple loading to complex loading, the explicit expression for α_{ij} should be given. α is defined as the angle between the directions of the deviator stress ratio tensor γ_{ij} and the incremental deviator stress ratio $d\gamma_{ij}$ at the n -th time step. Obviously α is the stress turning angle. Under simple loading, $\eta = (\gamma_{ij}\gamma_{ij})^{\frac{1}{2}} = \sqrt{2/3}q/p$. Taking the elements of the

tensor α_{ij} all equal to $\cos\alpha/3$, we can derive $\eta = \|\gamma_{ij}\| \cos\alpha/3$ under complex loading. η is always positive or equal to zero. The definition of stress turning angle α is given as

$$\cos\alpha = \frac{\sum[(\gamma_{ij}^n - \gamma_{ij0})d\gamma_{ij}^n]}{\left[\sum(\gamma_{ij}^n - \gamma_{ij0})^2 \sum(d\gamma_{ij}^n)^2\right]^{\frac{1}{2}}} \quad (i \leq j) \quad (9)$$

where γ_{ij0} is the initial deviator stress ratio. In order not to make the extended model complicated, the anisotropic hardening of γ_{ij0} is not considered. The value of α can be used as the criteria for judging the loading conditions under the complex loading. For example, when the stress turning angle α is $\alpha=0^\circ$, the soil is under a simple proportional loading; when $90^\circ < \alpha \leq 180^\circ$, the soil is under unloading conditions; when $0^\circ < \alpha < 90^\circ$, the soil is under a variable-stress-path loading.

The strain can be divided into quasi-elastic and plastic strains. The quasi-elastic strain is induced by the rolling or rotating of the soil skeletons, and the direction of the quasi-elastic strain is dependent on the stress increment. The plastic strain is induced by the sliding of the soil skeletons; the direction of the plastic strain is dependent on both the stress and the stress increment. Differentiating $\eta = \gamma_{ij}\alpha_{ij}$, we can get $d\eta = \alpha_{ij}d\gamma_{ij} + \gamma_{ij}d\alpha_{ij}$. At the n -th time step, we have only one stress turning of γ_{ij} and $d\gamma_{ij}$. It can be considered that $d\alpha_{ij} = 0$. Therefore we have $d\eta = \alpha_{ij}d\gamma_{ij}$.

Base on the above assumptions of quasi-elastic strain and plastic strain, the stress-strain relationship of soils under simple loading can be extended to the complicated loading case as

$$\begin{cases} d\varepsilon_v^e = A'dp' + Cw/(1-w)p'\alpha_{ij}d\gamma_{ij} \\ d\varepsilon_{ij}^e = B'dp'n_{1ij} + Dw/(1-w)p'n_{1ij}\alpha_{kl}d\gamma_{kl} \\ d\varepsilon_v^p = Ap'dp' + Cp'\alpha_{ij}d\gamma_{ij} \\ d\varepsilon_{ij}^p = Bp'dp'n_{2ij} + Dp'n_{ij}\alpha_{kl}d\gamma_{kl} \end{cases} \quad (10)$$

where $A = 1/(pK'_c)$, $B = \eta/(p\eta_oK'_c)$, $C = a\beta_2(1-w)(\eta_d - \eta)/(gp\lambda)$, $D = a(1-w)/(gp)$, $K'_c = K_cK_s/(K_s - K_c)$,

$$A' = 1/K_s, B' = \eta/(\eta_oK_s), g = (\eta_f - \eta)^2/\eta_f^2 + ac_f\eta(\eta_d - \eta)/(\eta_f^2\lambda), n_{1ij} = d\gamma_{ij}/(d\gamma_{ij}d\gamma_{ij})^{\frac{1}{2}},$$

$n_{2ij} = \gamma_{ij}/(\gamma_{ij}\gamma_{ij})^{\frac{1}{2}}$, $n_{ij} = n_{2ij}/3 + 2n_{1ij}/3$. β_2 is used for simulation of shearing induced contraction under inverse loading. $\beta_2 = 1$ when $\alpha_{ij}d\gamma_{ij} \geq 0$; $\beta_2 = -1$ when $\alpha_{ij}d\gamma_{ij} < 0$ and $\eta < \eta_d$. w is used to account for the proportionality of the quasi-elastic strain in the total strain and $w = g/2$.

It is worthy to note that, in the above hypo-plasticity model, the Macauley symbol ' $\langle \rangle$ ' is not included. Porewater pressure or volumetric strain will still be induced due to the natural structure under the compressive stress lower than the maximum stress in history. In the previous strain-porewater pressure type of model $\Delta u = E_{ur}\Delta\varepsilon_v$, the elastic rebounding modulus is adopted. Wang [13] rewrites the strain-porewater pressure type of model as $\Delta u = E_c\Delta\varepsilon_v$ using the compressive modulus. Shen [11] writes the

model as $\Delta u = \frac{E_{ur}}{b}\Delta\varepsilon_{vd}$ using a modulus value between E_c and E_{ur} , i.e., $E_c \leq \frac{E_{ur}}{b} \leq E_{ur}$. In

undrained condition, we have $d\varepsilon_v = d\varepsilon_v^e + d\varepsilon_v^p = 0$ and $du = -dp'$, therefore we can get the following relationship for the porewater pressure using the present hypo-plasticity model.

$$du = K_c \frac{\beta(\eta_d - \eta)}{\lambda} \frac{a}{g} \alpha_{ij} d\gamma_{ij} \quad (11)$$

The elastic strain can be written as

$$\begin{cases} d\varepsilon_v^e = \frac{1}{3K} dp \\ de_{ij}^e = \frac{1}{2G} ds_{ij} \end{cases} \quad (12)$$

where $\frac{1}{K} = \frac{1}{K_s} + \frac{aw}{g} \frac{\beta_2(\eta_d - \eta)}{\lambda} \frac{d\eta}{dp}$. Considering $d\gamma_{ij} = \frac{ds_{ij}}{p} - \frac{s_{ij}}{p^2} dp$, we can get the following relationship $\frac{1}{2G} = \left(\frac{dp}{d\eta} \frac{\eta}{\eta_o} \frac{1}{p} \frac{1}{K_s} + \frac{aw}{gp} \right) \left(1 - \frac{dp}{ds_{ij}} \frac{s_{ij}}{p} \right)$. It can be seen that the elastic moduli K and G are both dependent the stress path. For convenient use, K and G are usually taken as constant values.

The elastic stress-strain stiffness matrix is given in Eqn. (13) as

$$D_{ijkl}^e = K \delta_{ij} \delta_{kl} + G \left(\delta_{ik} \delta_{jl} + \delta_{il} \delta_{jk} - \frac{2}{3} \delta_{ij} \delta_{kl} \right) \quad (13)$$

Using $d\varepsilon_{ij}^p = \frac{1}{3} d\varepsilon_v^p \delta_{ij} + de_{ij}^p$, we can get

$$de_{ij}^p = \frac{1}{3} \frac{dp}{K_c} \delta_{ij} + \frac{1}{3} \frac{a(1-w)}{g} \frac{\beta_2(\eta_d - \eta)}{\lambda} d\eta \delta_{ij} + \frac{dp}{K_c} \frac{\eta}{\eta_o} n_{2ij} + \frac{a(1-w)}{g} n_{ij} d\eta \quad (14)$$

Using $d\varepsilon_{ij}^p = C_{ijkl}^p d\sigma_{kl}$, the plastic compliance matrix C_{ijkl}^p can be written as

$$\begin{aligned} C_{ijkl}^p &= \frac{1}{3K_c} \delta_{ij} \frac{\partial p}{\partial \sigma_{kl}} + \frac{1}{3} \frac{a(1-w)}{g} \frac{\beta_2(\eta_d - \eta)}{\lambda} \delta_{ij} \frac{\partial \eta}{\partial \sigma_{kl}} \\ &+ \frac{1}{K_c} \frac{\eta}{\eta_o} n_{2ij} \frac{\partial p}{\partial \sigma_{kl}} + \frac{a}{g} (1-w) n_{ij} \frac{\partial \eta}{\partial \sigma_{kl}} \\ &= \left(\frac{1}{9} \delta_{ij} + \frac{\eta}{3\eta_o} n_{2ij} \right) \frac{\delta_{kl}}{K_c} + \left[\frac{\beta_2(\eta_d - \eta)}{3\lambda} \delta_{ij} + n_{ij} \right] \frac{a(1-w)}{g} \frac{\partial \eta}{\partial \sigma_{kl}} \end{aligned} \quad (15)$$

Eqn. (16) gives a series of elasto-plastic stress-strain relationships.

$$\begin{cases} d\varepsilon_{ij}^e = D_{ijkl}^{e-1} d\sigma_{kl} \\ d\varepsilon_{ij}^p = C_{ijkl}^p d\sigma_{kl} \\ d\varepsilon_{ij} = D_{ijkl}^{ep-1} d\sigma_{kl} \\ d\varepsilon_{ij}^e = d\varepsilon_{ij} - d\varepsilon_{ij}^p \\ d\sigma_{ij} = \left(I_{ijmn} + D_{ijkl}^e C_{klmn}^p \right)^{-1} D_{mnl}^e d\varepsilon_{kl} \end{cases} \quad (16)$$

By means of the relationships in Eqn. (16), the elasto-plastic stress-strain stiffness matrix D_{ijkl}^{ep} can be written as

$$D_{ijkl}^{ep} = \left(I_{ijmn} + D_{ijkl}^e C_{klmn}^p \right)^{-1} D_{mnl}^e \quad (17)$$

where I_{ijmn} are the unit matrix.

We can also derive another expression of the elastic plastic stiffness matrix D_{ijkl}^{ep} using the present hypo-plasticity model as following

$$D_{ijkl}^{ep} = D_{ijkl}^e - M_{ijkl} / H \quad (18a)$$

$$M_{ijkl} = 2GD \left[\left(\frac{1}{K} + A \right) n_{ij} \alpha_{kl} - \left(\frac{1}{2G} + B \right) (n_{2ij} \alpha_{ij}) n_{ij} \delta_{kl} \right] \\ + CK \left[\left(\frac{1}{K} + A \right) \delta_{ij} \alpha_{kl} - \left(\frac{1}{2G} + B \right) (n_{2ij} \alpha_{ij}) \delta_{ij} \delta_{kl} \right] \quad (18b)$$

$$- 2GB \left[C n_{2ij} \alpha_{kl} - \left(\frac{1}{2G} + D n_{ij} \alpha_{ij} \right) n_{2ij} \delta_{kl} \right] \\ - AK \left[C \delta_{ij} \alpha_{kl} - \left(\frac{1}{2G} + D n_{ij} \alpha_{ij} \right) \delta_{ij} \delta_{kl} \right] \\ H = \left(\frac{1}{2G} + D n_{ij} \alpha_{ij} \right) \left(\frac{1}{K} + A \right) - C \left(\frac{1}{2G} + B \right) n_{2ij} \alpha_{ij} \quad (18c)$$

The symbols such as A , B , C and D in Eqn. (18) are the same as those in Eqn. (10) and have been defined and explained above.

Using the parameters in Tab. 1, the present hypo-plasticity model is used to predict the test results from drained triaxial cyclic shear tests under constant confining pressure and under constant mean pressure. The predicted results and the measured results are shown in Figs. 1 (a) and (b). The simple computational example gives a preliminary verification of the present hypo-plasticity model.

Tab. 1 The parameters of the silty clay for the triaxial tests modeling

η_f	η_d	c_c	c_s	a	λ	c_f	η_o
1.0	0.9	0.15	0.015	0.025	1.0	1.5	0.65

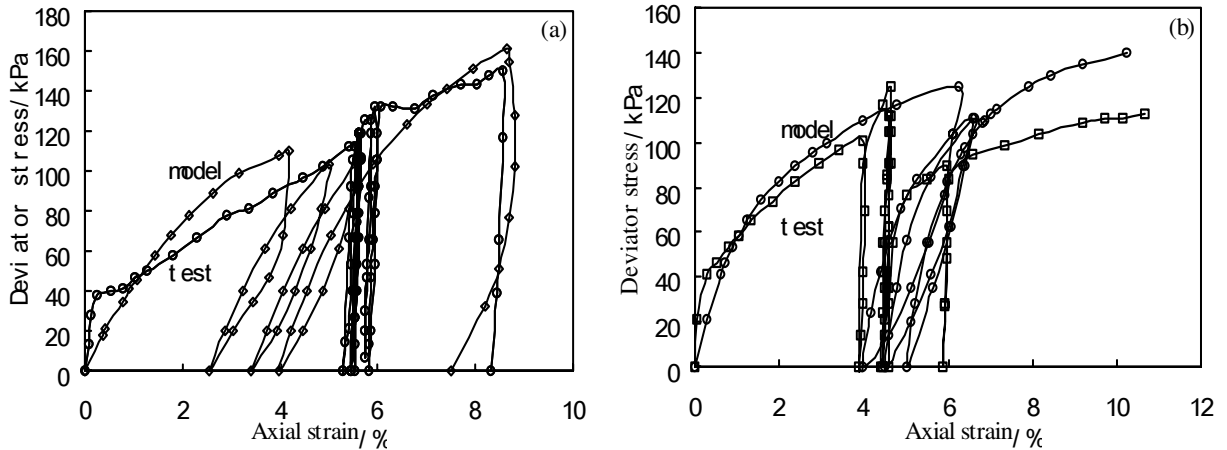


Fig. 1 The simulation of hypoplasticity model of the drained triaxial cyclic shear tests on silty clay under (a) constant confining pressure $\sigma_3=100$ kPa and (b) constant mean pressure $p=100$ kPa

THE ASYNCHRONOUS STAGGERED ITERATION METHOD WITH AN EXPLICIT DIFFERENCE SCHEME

In the equivalent viscous elastic analysis method, the plastic strains are considered as equivalent viscous strains and an empirical damping term is included. In the elastic plastic analysis, the tangent stiffness matrix is formulated by using elastic plastic or hypo-plastic models, and the empirical damping term is not used again. The finite element governing equation of the Biot dynamic consolidation theory in Eqn. (19) can be used to solve the deformation of soil skeletons and the porewater pressure.

$$\begin{cases} [M] \{\ddot{u}\} + [K] \{u\} + [C] \{P\} = \{F_1\} \\ [A] \{\ddot{u}\} + [C^T] \{\dot{u}\} + [S] \{\dot{P}\} + [H] \{P\} = \{F_2\} \end{cases} \quad (19)$$

where $[M]$ is the mass matrix, $[K]$ is the stiffness matrix, $[C]$ is the coupling matrix, $[H]$ is the permeability matrix, $[A]$ and $[S]$ are the inertial matrix and compressibility matrix of the liquid. $\{F_1\}$ is the loading vector matrix, $\{F_2\}$ is the flowing vector matrix. If the compressibility and the empirical force of the liquid are ignored, Eqn. (19) can be written as following

$$\begin{cases} [M] \{\ddot{u}\} + [K] \{u\} + [C] \{P\} = \{F_1\} \\ [C^T] \{\dot{u}\} + [H] \{P\} = \{F_2\} \end{cases} \quad \text{£}^{\circ}20\text{£}^{\circ}$$

If the frequency of the wave is very small, the inertial force of the soil skeletons can be further ignored, the finite element governing equation of the Biot static consolidation theory can be derived as the following

$$\begin{cases} [K] \{\Delta u\} + [C] \{P\} = \{\bar{F}_1\} \\ [C^T] \{\Delta u\} + \Delta t [H] \{P\} = \{\bar{F}_2\} \end{cases} \quad (21)$$

It is obvious that the permeability continuum equation is the same in Eqns. (20) and (21). In comparison with the Biot static consolidation equation, the key issue of the solution of the Biot dynamic consolidation equation is how to solve the dynamic equilibrium equation and correctly couple it with the permeability continuum equation. We can adopt an explicit finite difference scheme and Newmark integration scheme for elasto-plastic analyses, so that the deformation and porewater pressure in each time step Δt can be solved staggeredly. However, the explicit finite difference scheme is conditionally stable. Δt should be small enough and at least less than the period that stress wave propagates in an element. The compressive modulus of water is larger than 2500Mpa and thus Δt is at least between 0.0001 and 0.001 second. If we consider further the requirement of permeability of various soils and iteration convergence, Δt will be smaller. Thus, Δt can reach the requirement of stability of the explicit finite difference scheme in equilibrium equation, but it can not satisfy the requirement of permeability continuum equation about Δt . According to the experience of finite element analyses of the Biot static consolidation equation, if Δt is too small, $\Delta t [H]$ in the permeability continuum equation will be so small that the elements on the diagonal line of the matrix corresponding to $\{P\}$ vector matrix will be too small and the coefficient matrix in the process of solution will be in ill condition. Therefore, in the Biot static consolidation analyses $\Delta t = \theta L^2 / C_v$ ($\theta = 0.25 \sim 1$, L is the size of the mesh, and C_v is the coefficient of consolidation)[2,7]. If Δt is determined for the stability of explicit finite difference scheme in equilibrium equation, the value of Δt will be much smaller than that derived from $\Delta t = \theta L^2 / C_v$.

In order to satisfy the different requirements of Δt for both the explicit finite difference scheme in the Biot dynamic equilibrium equation and the permeability continuum equation, an asynchronous staggered iteration method with an explicit difference scheme is suggested in this paper. Assuming that the

deformation and porewater pressure at time step (n+1)-th, n-th, (n-1)-th are $\{u_{n+1}\}$, $\{u_n\}$, $\{u_{n-1}\}$ and $\{P_{n+1}\}$, $\{P_n\}$, $\{P_{n-1}\}$ respectively, we can use central difference scheme in Eqn. (22) to derive the following Eqn. (23):

$$\begin{aligned} \{\ddot{u}_{n+1}\} &= [\{u_{n+1}\} - 2\{u_n\} + \{u_{n-1}\}]/(\Delta t^2) & \text{£}22\text{£} \odot \\ \{u\}_{n+1} &= 2\{u\}_n - \{u\}_{n-1} + [M]^{-1} (\{F_1\}_n - [C]\{P\}_n - [K]\{u\}_n)\Delta t^2 & \text{£}23\text{£} \odot \end{aligned}$$

Due to that $[M]$ is a symmetric matrix about the diagonal line and there are only constant elements on the diagonal line, the inverse matrix of $[M]$ can be derived for one time and kept constant at all time steps. We can solve $\{u\}_{n+1}$ from Eqn. (23), and substitute it into Eqn. (22) to derive $\{\dot{u}\}_{n+1}$. Using Newmark integration scheme we can express $\{\dot{u}\}_{n+1}$ and $\{P\}_{n+1}$ as

$$\begin{cases} \{\dot{u}\}_{n+1} = \alpha \Delta t \{\ddot{u}\}_{n+1} + \{A\}_n \\ \{P\}_{n+1} = \gamma \Delta t \{\dot{P}\}_{n+1} + \{B\}_n \end{cases} \quad \text{£}24\text{£} \odot$$

where $\{A\}_n = \{\dot{u}\}_n + (1 - \alpha)\Delta t \{\ddot{u}\}_n$ and $\{B\}_n = \{P\}_n + (1 - \gamma)\Delta t \{\dot{P}\}_n$. Thus the permeability continuum equation in Eqn. (20) can be written as

$$\gamma \Delta t [H] \{\dot{P}\}_{n+1} = \{F_2\}_{n+1} - [C^T] \{A\}_n - [H] \{B\}_n - \alpha \Delta t [C^T] \{\ddot{u}\}_{n+1} \quad (25)$$

Substituting the derived $\{\dot{u}\}_{n+1}$ into Eqn. (25), we can derive $\{\dot{P}\}_{n+1}$. However, due to the reason that too small Δt will make $\Delta t [H]$ in ill condition, the staggered iterative solutions of Eqns. (25) and (23) will be asynchronous. When we use $\{P\}_n$ to derive $\{u\}_{n+1}$ in Eqn. (23), $\{P\}_n$ at this instant moment is assumed to be constant since the time interval is very small. $\{u\}_n$ and $\{u\}_{n-1}$ at next time steps are used to derive $\{u\}_{n+1}$ continuously until the accumulated time interval is enough to make $\Delta t [H]$ in Eqn. (25) not in ill condition again and $\{\dot{P}\}_{n+1}$ can be solved. Substituting derived $\{\dot{P}\}_{n+1}$ into Eqn. (24), we can derive $\{P\}_{n+1}$.

It can be found that the time interval in asynchronous staggered iteration is also related to the permeability coefficient of soils. When the permeability coefficient is large, the asynchronous staggered iteration may almost recover to synchronous staggered iteration. However, when the permeability coefficient is small, the asynchronous staggered iteration method is better to be adopted. In addition, in the adopted hypo-plasticity model, the magnitude and direction of the plastic strain is dependent not only on the magnitude and direction of the total stress, but also on those of the stress increment. Therefore, in the solid-liquid coupling finite element analysis, the current magnitude and direction of the stress increment should be previously determined by elastic modelling, then the elastic plastic analysis is conducted to determine the magnitude and direction of the stress increment in next step. The staggered iteration method is repeated until the convergence is reached. The newly determined magnitude and direction of the total stress will be taken as the initial values for the next step.

FINITE ELEMENT ANALYSES

The dynamic solid-liquid coupling elasto-plastic responses of a saturated sand foundation are analyzed using the present hypo-plasticity model and asynchronous staggered iteration method with an explicit difference scheme. The model parameters for the analysis are listed in Tab. 2. The input horizontal acceleration is a regular sine wave with 1Hz frequency. The maximum acceleration is 0.1g. The foundation is divided into a zone with a mesh of 20 joints and 12 four-joint isoparametric element, as shown in Fig. 2. The mesh size is $3m \times 2m$. The simple left and right manual boundaries are horizontally constrained only and closed to drainage. The simple bottom manual boundary is vertically constrained only and also closed to drainage. The top surface is free to deformation and drainage. The asynchronous staggered iterative time interval is $30 \Delta t = 3 \times 10^{-4}$ second. Figs. 3 and 4 show the computed results of

lateral displacement, vertical settlement and porewater pressure of the 10-*th* joint at time $t=10$ seconds. It can be found from Figs. 3 and 4 that, the lateral displacement, vertical displacement and porewater pressure all exhibit vibrating characteristics due to the input cyclic sine wave. Although the peak values of the porewater pressure at some time steps are negative, the most peak values are positive and the absolute values are relatively larger than others. The horizontal displacement turns from negative values to positive values progressively in the process of vibration, and the positive values are absolutely larger. The values of vertical settlement are positive in general. The computed results are generally reasonable. However, there are still some limitation of the adopted hypo-plasticity model and numerical solution methods, such as asynchronous staggered iteration of deformation and porewater pressure, and staggered iteration of elasticity model and hypo-plasticity model.

Tab.2 The parameters of sand for the hypo-plasticity model in finite element analysis

η_f	η_d	c_c	c_s	a	λ	c_f	η_o
1.58	0.89	0.0048	0.001	0.0023	0.6	1.5	0.75

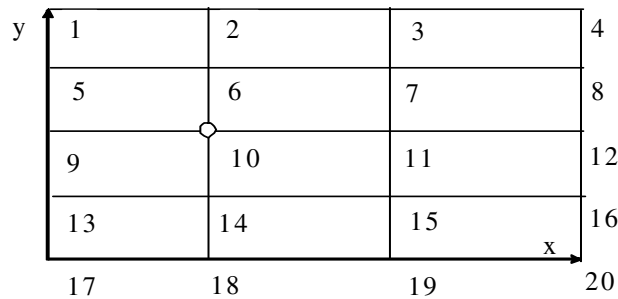


Fig. 2 The grid of the sand ground in the dynamic finite element analysis (element size: 3m x 2m)

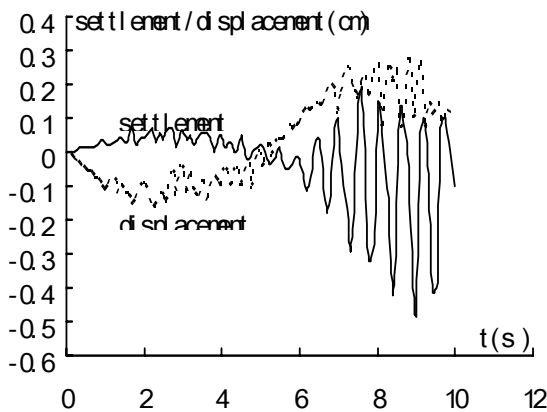


Fig. 3 Horizontal displacement and vertical settlement of 10-*th* joint vs. time in vibration

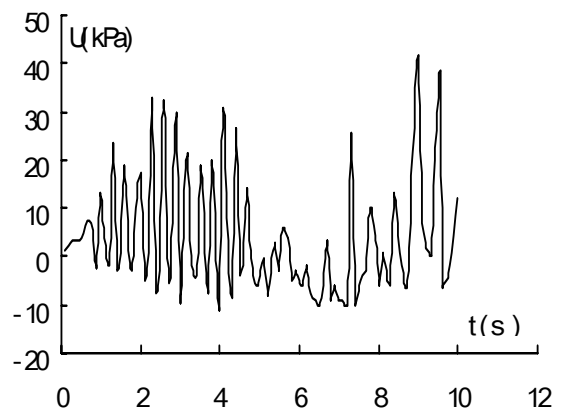


Fig. 4 Porewater pressure of 10-*th* joint vs. time in vibration

CONCLUSIONS

A hypo-plasticity model is presented and preliminarily verified using triaxial tests on silty clays. An asynchronous staggered iteration method with an explicit difference scheme is suggested. The algorithm and the hypo-plasticity model are implemented in a finite element (FE) code based on Biot dynamic consolidation theory. The presented algorithm can make the coefficient matrix $\Delta t [H]$ not in ill condition when decoupling the dynamic equilibrium equation and the permeability continuum equation with a very small Δt . The staggered iteration between the elastic model and the hypo-plasticity model makes it possible to determine the stress increment previously for the hypo-plasticity model in finite element analysis. The dynamic solid-liquid coupling elasto-plastic responses of a saturated sand foundation are analyzed and reasonable results are achieved.

ACKNOWLEDGEMENTS

The preparation of this paper has received financial supports from a RGC grant (PolyU 5041/01E) of the University Grants Committee of the Hong Kong SAR Government of China. The financial support is gratefully acknowledged.

REFERENCES

1. Shen ZJ. "Theoretical soil mechanics." Beijing, China: China Hydropower Publishing House, 2000 (in Chinese).
2. Zhu BL and Shen ZJ. "Computational soil mechanics." Shanghai, China: Shanghai Science and Technology Publishing House, 1990 (in Chinese).
3. Ishihara K. Analysis of wave-induced liquefaction in seabed deposits of sand." Soils and Foundations 1984; 24(3).
4. Zhou C, Shen ZJ, Chen SS and Yin JH. "Hypo-plasticity model and analysis of dynamic elasto-plastic response of saturated sand." Rock and Soil Mechanics 2004; 25(4). (in Chinese)
5. Zhou C, Shen ZJ, Yin JH and Chen SS. "Solution to Biot solid-liquid coupling dynamic consolidation equation using an asynchronous staggered iteration finite element method with explicit difference scheme." Proceedings of the 9th National Conference on Soil Mechanics and Geotechnical Engineering. Beijing, China: The Publishing House of Tsinghua University, 2003: 1061-1064 (in Chinese).
6. Zhou C, Shen ZJ, Li NH and Chen SS. "Constitutive model of structured soil and elasto-plastic damaging analysis of solid-liquid coupling dynamic problem." Journal of Hydro-science and Engineering 2003; 3: 1-6 (In Chinese).
7. Zhou C. "Constitutive model of structured soil and numerical analyses." PhD thesis. Nanjing, China: Nanjing Hydraulic Research Institute, 2002 (in Chinese).
8. Wang ZL, Dafalias YF and Shen CK. "Bounding surface hypoplasticity model for sands." ASCE Journal of Engineering Mechanics 1990; 116(5): 983-1001.
9. Chen SS, Shen ZJ and Li NH. "Elastic plastic numerical simulation of cohesiveless soils under complex stress path." Chinese Journal of Geotechnical Engineering 1995; 17(2): 20-28 (in Chinese).
10. Shen ZJ. "A granular medium model for liquefaction analysis of sands." Chinese Journal of Geotechnical Engineering 1999; 21(6): 742-748 (in English).
11. Shen ZJ. "Liquefied deformation and structure model of sand under complex loading." Proceedings of 5th National Conference on Dynamic Soil Mechanics, China, Dalian: The Publishing House of Dalian University of Technology, 1998: 1-10 (in Chinese).
12. Zhou C, Shen ZJ, Chen SS and Yin JH. "Elasto-plastic analysis for structured soils under complex loading." Adachi and Fukue, Editors. Clay Science for Engineering. Rotterdam:AA Balkema, 2001: 459-466.

13. Wang WS. "Laboratory study on the dynamic porewater pressure of saturated sand." Journal of Hydraulic Science and Engineering 1968 (2): (in Chinese).